

$\chi^{(2)}$ and $\chi^{(3)}$ harmonic generation at a critical power in inhomogeneous doubly resonant cavities

Alejandro Rodriguez, Marin Soljačić, J. D. Joannopoulos, and Steven G. Johnson¹

¹*Center for Materials Science and Engineering, Massachusetts Institute of Technology, Cambridge, MA 02139**

We derive general conditions for 100% frequency conversion in any doubly resonant nonlinear cavity, for both second- and third-harmonic generation via $\chi^{(2)}$ and $\chi^{(3)}$ nonlinearities. We find that conversion efficiency is optimized for a certain “critical” power depending on the cavity parameters, and assuming reasonable parameters we predict 100% conversion using milliwatts of power or less. These results follow from a semi-analytical coupled-mode theory framework which is generalized from previous work to include both $\chi^{(2)}$ and $\chi^{(3)}$ media as well as inhomogeneous (fully vectorial) cavities, analyzed in the high-efficiency limit where down-conversion processes lead to a maximum efficiency at the critical power, and which is verified by direct finite-difference time-domain (FDTD) simulations of the nonlinear Maxwell equations. Explicit formulas for the nonlinear coupling coefficients are derived in terms of the linear cavity eigenmodes, which can be used to design and evaluate cavities in arbitrary geometries.

PACS numbers:

INTRODUCTION

In this paper, we consider second- and third-harmonic generation in doubly resonant cavities. We generalize previous experimental and theoretical work on this subject, which had focused only on $\chi^{(2)}$ nonlinearities in large Fabry-Perot etalons or two-dimensional ring resonators where a scalar approximation applied [1, 2, 3, 4, 5, 6, 7, 8, 9], to incorporate both $\chi^{(2)}$ and $\chi^{(3)}$ nonlinearities and handle the inhomogeneous fully vectorial case. We then develop several results from this generalization: whereas it is well known that 100% harmonic conversion is possible, at least in $\chi^{(2)}$ media, in this work we further explore and identify the conditions under which this can be achieved. First, we demonstrate the existence of a critical input power at which harmonic generation is maximized, in contrast to previous work that focused largely on the low-power limit in which generation efficiency increased monotonically with input power [3]. Second, while it is well known that harmonic conversion can be achieved at arbitrarily low powers given sufficiently long cavity lifetimes, this implies a narrow bandwidth—we show that, by combining moderate lifetimes (0.1% bandwidth) with tight spatial confinement, 100% second- and third-harmonic conversion can theoretically be achieved with sub-milliwatt power levels. Such low-power conversion could find applications such as high-frequency sources [5], ultracompact-coherent optical sources [10, 11, 12], imaging [13], and spectroscopy [14].

Nonlinear frequency conversion has been commonly realized in the context of waveguides [15, 16, 17, 18], or even for free propagation in the nonlinear materials, in which light at one frequency co-propagates with the generated light at the harmonic frequency [19, 20, 21, 22]. A phase-matching condition between the two frequencies must be satisfied in this case in order to obtain ef-

ficient conversion [5, 9]. Moreover, as the input power is increased, the frequency conversion eventually saturates due to competition between up and down conversion. Frequency conversion in a doubly resonant cavity has three fundamental differences from this familiar case of propagating modes. First, light in a cavity can be much more intense for the same input power, because of the spatial (modal volume V) and temporal (lifetime Q) confinement. We show that this enhances second-harmonic ($\chi^{(2)}$) conversion by a factor of Q^3/V and enhances third-harmonic ($\chi^{(3)}$) conversion by a factor of Q^2/V . Second, there is no phase-matching condition per se for 100% conversion; the only absolute requirement is that the cavity support two modes of the requisite frequencies. However, there is a constant factor in the power that is determined by an overlap integral between the mode field patterns; in the limit of a very large cavity, this overlap integral recovers the phase-matching condition for $\chi^{(2)}$ processes. Third, the frequency conversion no longer saturates—instead, it peaks (at 100%, with proper design) for a certain critical input power satisfying a resonant condition, and goes to *zero* if the power is *either* too small or too large.

Second-harmonic generation in cavities with a single resonant mode at the pump frequency [10, 14, 23, 24, 25, 26, 27, 28, 29, 30, 31, 32, 33, 34, 35, 36, 37, 38] or the harmonic frequency [39] requires much higher power than a doubly resonant cavity, approaching one Watt [3, 38] and/or requiring amplification within the cavity. (A closely related case is that of sum-frequency generation in a cavity resonant at the two frequencies being summed [40].) Second-harmonic generation in a doubly resonant cavity, with a resonance at both the pump and harmonic frequencies, has most commonly been analyzed in the low-efficiency limit where nonlinear down-conversion can be neglected [4, 5, 6, 7, 8, 9], but down-conversion has also been included by some au-

thors [1, 2, 3]. Here, we show that not only is down-conversion impossible to neglect at high conversion efficiencies (and is, in fact, necessary to conserve energy), but also that it leads to a critical power where harmonic conversion is maximized. This critical power was demonstrated numerically by Ref. 41 in a sub-optimal geometry where 100% efficiency is impossible, but does not seem to have been clearly explained theoretically; the phenomenon (for $\chi^{(2)}$) was also implicit in the equations of Ref. 3 but was not identified, probably because it occurred just beyond the range of power considered in that work.

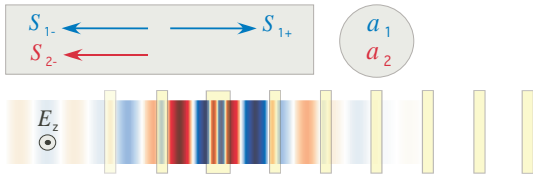


FIG. 1: *Top*: Schematic diagram of waveguide-cavity system. Input light from a waveguide (left) at one frequency (amplitude s_{1+}) is coupled to a cavity mode (amplitude a_1), converted to a cavity mode at another frequency (amplitude a_2) by a nonlinear process, and radiated back into the waveguide (amplitude s_{2-}). Reflections at the first frequency (s_{1-}) may also occur. *Bottom*: 1d example, formed by quarter-wave defect in a quarter-wave dielectric stack. Dielectric material is yellow, and electric field E_z of third-harmonic mode is shown as blue/white/red for positive/zero/negative amplitude.

Previous work on third-harmonic generation in cavities considered only singly resonant cavities; moreover, past work focused on the case of $\chi^{(2)}$ materials where 3ω is generated by cascading two nonlinear processes (harmonic generation and frequency summing) [14, 42]. Here, we examine third-harmonic generation using $\chi^{(3)}$ materials so that only a single resonant process need be designed and a different set of materials becomes available. ($\chi^{(3)}$ third-harmonic generation in a bulk periodic structure, with no cavity, was considered in Ref. 43.) In a $\chi^{(3)}$ medium, there are also self/cross-phase modulation phenomena (nonlinear frequency shifts) that, unchecked, will prevent 100% conversion by making the frequency ratio $\neq 3$. To address this mismatch, we describe how one can use two materials with opposite-sign $\chi^{(3)}$ to cancel the frequency-shifting effect; it may also be possible to pre-shift the cavity resonant frequency to correct for the nonlinear shift. On the other hand, a $\chi^{(2)}$ medium has no self-phase modulation, and so in this case it is sufficient to increase the input power until 100% frequency conversion is reached. (An “effective” self-phase modulation occurs in $\chi^{(2)}$ media due to cascaded up- and down-conversion processes [44], but these processes are fully taken into account by our model. We also consider media with simultaneous $\chi^{(2)}$ and $\chi^{(3)}$ nonlinearities, and show that the latter can be made negligible.) If the critical field were too intense, then material breakdown might

also be an obstacle, but we show that it is sufficient to use modes with a large lifetime Q and small volume V so that a slow conversion due to a weak nonlinear effect has enough time to occur.

In particular, we consider the general situation depicted schematically in Fig. 1: a two-mode nonlinear cavity coupled to an input/output channel. For example, a one-dimensional realization of this is shown in Fig. 1: a Fabry-Perot cavity between two quarter-wave stacks [45], where the stack has fewer layers on one side so that light can enter/escape. For a nonlinear effect, we consider specifically a $\chi^{(\ell)}$ nonlinearity, corresponding essentially to a shift in the refractive index proportional to the nonlinear susceptibility $\chi^{(\ell)}$ multiplied by electric field \mathbf{E} to the $(\ell - 1)^{th}$ power. Most commonly, one would have either a $\chi^{(2)}$ (Pockels) or $\chi^{(3)}$ (Kerr) effect. Such a nonlinearity results in harmonic generation [46]: light with frequency ω is coupled to light with frequency $\ell\omega$. Therefore, if we design the cavity so that it supports two modes, one at ω and one at $\ell\omega$, then input power at ω can be converted, at least partially, to output power at $\ell\omega$.

In the following, we derive a semi-analytical description of harmonic generation using the framework of coupled-mode theory [1, 2, 3, 5, 9, 10, 14, 31, 37, 47], and then check it via direct numerical simulation of the nonlinear Maxwell equations [7, 48, 49]. For maximum generality, we derive the coupled-mode equations using two complementary approaches. First, we use “temporal” coupled-mode theory [50, 51], in which the general form of the equations is determined only from principles such as conservation of energy and reciprocity, independent of the specific physical problem (for example, electromagnetic or acoustic waves). Second, we apply perturbation theory directly to Maxwell’s equations in order to obtain the same equations but with specific formulas for the coupling coefficients in terms of the linear eigenmodes. Unlike most previous treatments of this problem [1, 2, 47], we do not make a one-dimensional or scalar approximation for the electromagnetic fields (invalid for wavelength-scale cavities), and we consider both $\chi^{(2)}$ and $\chi^{(3)}$ media. (The optimization of these coupling coefficients is then the generalization of the phase-matching criteria used in one-dimensional geometries [5].)

TEMPORAL COUPLED-MODE THEORY

We derive coupled-mode equations describing the interaction of light in a multi-mode cavity filled with nonlinear material and coupled to input/output ports, from which light can couple in (s_+) and out (s_-) of the cavity. A schematic illustration of the system is shown in Fig. 1. Specifically, we follow the formalism described in Ref. 50, adapted to handle nonlinearly coupled modes with frequencies ω_k . Although similar equations for the case of $\chi^{(2)}$ media were derived in the past [3], they do

not seem to have been derived for $\chi^{(3)}$ harmonic generation in cavities. Moreover, a derivation via the temporal coupled-mode formalism of Ref. 50 is arguably more general than earlier developments based on a particular scalar nonlinear wave equation, because this formalism (for a given-order nonlinearity) depends only on general considerations such as weak coupling and energy conservation (the resulting equations hold for vector or scalar waves in electromagnetism, acoustics, or any other weakly-coupled problem with a few simple properties). In the next section, we will then specialize the equations to electromagnetism by deriving explicit equations for the coupling coefficients from Maxwell's equations.

We let a_k denote the time-dependent complex amplitude of the k th mode, normalized so that $|a_k|^2$ is the electromagnetic energy stored in this mode. We let s_{\pm} denote the time-dependent amplitude of the incoming (+) or outgoing (−) wave, normalized so that $|s_{\pm}|^2$ is the power. (More precisely, $s_{\pm}(t)$ is normalized so that its Fourier transform $|\tilde{s}_{\pm}(\omega)|^2$ is the power at ω . Later, we will let $s_{k\pm}$ denote the input/output power at ω_k .) [In 1d, the units of $|a_k|^2$ and $|s_{\pm}|^2$ are those of energy and power per unit area, respectively. More generally, in d dimensions, the units of $|a_k|^2$ and $|s_{\pm}|^2$ are those of energy and power per length $^{3-d}$.] By itself, a linear cavity mode decaying with a lifetime τ_k would be described by $da_k/dt = (i\omega_k - 1/\tau_k)a_k$. [Technically, such a decaying mode is not a true eigenmode, but is rather a “leaky mode” [52], corresponding to a “quasi-bound state” in the Breit-Wigner scattering theory [53].] The decay rate $1/\tau_k$ can be decomposed into $1/\tau_k = 1/\tau_{e,k} + 1/\tau_{s,k}$ where $1/\tau_{e,k}$ is the “external” loss rate (absorption etc.) and $1/\tau_{s,k}$ is the decay rate into s_- . When the weak coupling ($\omega_k\tau_k \gg 1$) to s_{\pm} is included, energy conservation and similar fundamental constraints lead to equations of the form [54]:

$$\frac{da_k}{dt} = \left(i\omega_k - \frac{1}{\tau_k}\right) a_k + \sqrt{\frac{2}{\tau_{s,k}}} s_+ \quad (1)$$

$$s_- = -s_+ + \sqrt{\frac{2}{\tau_{s,k}}} a_k \quad (2)$$

This can be generalized to incorporate multiple input/output ports, direct coupling between the ports, and so on [51]. The only unknown parameters in this model are then the frequencies ω_k and the decay rates $1/\tau_k$, which can be determined by any numerical method to solve for the cavity modes (e.g. FDTD, below). Instead of τ_k , one commonly uses the quality factor $Q_k = \omega_k\tau_k/2$.

Nonlinearity modifies this picture with two new amplitude-dependent effects: a shift in the frequency (and decay rate) of the cavity, and a coupling of one cavity mode to another. We neglect nonlinear effects on the input/output ports, under the assumption that intense fields are only present in the cavity (due to spatial and temporal confinement). We will also make two standard assumptions of nonlinear systems. First, that the nonlinearities are weak, in the sense that we can neglect terms of order $(\chi^{(\ell)})^2$ or higher; this is true in practice because nonlinear index shifts are always under 1% lest material breakdown occur. Second, we make the rotating wave approximation: since the coupling is weak, we only include terms for a_k that have frequency near ω_k . In particular, we suppose that $\omega_k \approx k\omega_1$, so that ω_k is the k th harmonic. The result is that, for a given order nonlinearity, there are only a few possible new terms that can appear in the coupled-mode equations. In particular, for a $\chi^{(2)}$ nonlinearity with two modes ω_1 and its second harmonic ω_2 , the coupled-mode equations must take the form:

$$\frac{da_1}{dt} = \left(i\omega_1 - \frac{1}{\tau_1}\right) a_1 - i\omega_1\beta_1 a_1^* a_2 + \sqrt{\frac{2}{\tau_{s,1}}} s_+ \quad (3)$$

$$\frac{da_2}{dt} = \left(i\omega_2 - \frac{1}{\tau_2}\right) a_2 - i\omega_2\beta_2 a_1^2 + \sqrt{\frac{2}{\tau_{s,2}}} s_+ \quad (4)$$

Similarly, for a $\chi^{(3)}$ nonlinearity with two modes ω_1 and its third harmonic ω_3 , the coupled-mode equations must take the form:

$$\frac{da_1}{dt} = \left(i\omega_1(1 - \alpha_{11}|a_1|^2 - \alpha_{13}|a_3|^2) - \frac{1}{\tau_1}\right) a_1 - i\omega_1\beta_1(a_1^*)^2 a_3 + \sqrt{\frac{2}{\tau_{s,1}}} s_+ \quad (5)$$

$$\frac{da_3}{dt} = \left(i\omega_3(1 - \alpha_{33}|a_3|^2 - \alpha_{31}|a_1|^2) - \frac{1}{\tau_3}\right) a_3 - i\omega_3\beta_3 a_1^3 + \sqrt{\frac{2}{\tau_{s,3}}} s_+ \quad (6)$$

In equations 5–6, one sees two kinds of terms. The first

are *frequency-shifting* terms, with coefficients α_{ij} , depen-

dent on one of the field amplitudes. For $\chi^{(3)}$, this effect is known as self-phase and cross-phase modulation, which is absent for $\chi^{(2)}$ (under the first-order rotating-wave approximation). The second kind of term *transfers energy* between the modes, with coupling coefficients β_i , corresponding to four-wave mixing for $\chi^{(3)}$. Furthermore, we can constrain the coupling terms β_i by energy conservation: $\frac{d}{dt}(|a_1|^2 + |a_2|^2) = 0$. For $\chi^{(2)}$, the constraint that follows is: $\omega_1\beta_1 = \omega_2\beta_2^*$; for $\chi^{(3)}$, the constraint is $\omega_1\beta_1 = \omega_3\beta_3^*$. (This constraint holds even in cavities with external loss as discussed in Sec. : energy is still conserved in the sense that the input power must equal the output power plus the loss power, and so the harmonic conversion term must lead to an equal energy loss and gain at ω_1 and $\omega_{2,3}$, respectively.)

The general process for construction of these coupled-mode equations is as follows. The underlying nonlinearity must depend on the physical, real part of the fields, corresponding to $(a_k + a_k^*)/2$. It then follows that the $\chi^{(\ell)}$ term will have ℓ powers of this real part, giving various product terms like $a_1^*a_2$ (for $\chi^{(2)}$) and $a_1^*a_1a_1$ (for $\chi^{(3)}$). Most of these terms, however, can be eliminated by the rotating-wave approximation. In particular, we assume that each a_k term is proportional to $e^{ki\omega}$ multiplied by a slowly varying envelope, and we discard any product term whose total frequency differs from $k\omega$ for the da_k/dt equation. Thus, a term like $a_1^*a_3a_3$ would be proportional to $e^{5i\omega}$, and would only appear in a da_5/dt equation. (We focus on the simpler case of doubly resonant cavities in this paper.)

At this point, the equations are already useful in order to reason about what types of qualitative behaviors are possible in general. In fact, they are not even specific to electromagnetism and would also apply to other situations such as acoustic resonators. However, in order to make quantitative predictions, one needs to know the nonlinear coefficients α_{ij} and β_i (as well as the linear frequencies and decay rates). The evaluation of these coefficients requires a more detailed analysis of Maxwell's equations as described below.

PERTURBATION THEORY AND COUPLING COEFFICIENTS

In this section, we derive explicit formulas for the nonlinear coupling coefficients in the coupled-mode theory of the previous section, applied to the case of electromagnetism. Unlike previous work, our expressions apply to

the fully vectorial equations, valid for high index-contrast materials, and we derive the $\chi^{(3)}$ case as well as $\chi^{(2)}$. Our derivation is closely related to that of Ref. 55, which only considered the frequency shifting (self-phase modulation) and not harmonic generation.

When a dielectric structure is perturbed by a small $\delta\varepsilon$, a well-known result of perturbation theory states that the corresponding change $\delta\omega$ in an eigenfrequency ω is, to first order [45]:

$$\frac{\delta\omega}{\omega} = -\frac{1}{2} \frac{\int d^3\mathbf{x} \delta\varepsilon |\mathbf{E}|^2}{\int d^3\mathbf{x} \varepsilon |\mathbf{E}|^2} = -\frac{1}{2} \frac{\int d^3\mathbf{x} \mathbf{E}^* \cdot \delta\mathbf{P}}{\int d^3\mathbf{x} \varepsilon |\mathbf{E}|^2} \quad (7)$$

where \mathbf{E} is the unperturbed electric field and $\delta\mathbf{P} = \delta\varepsilon\mathbf{E}$ is the change in polarization density due to $\delta\varepsilon$. In fact, Eq. 7 is general enough to be used with any $\delta\mathbf{P}$, including the polarization that arises from a nonlinear susceptibility. In particular, we can use it to obtain the coupling coefficients of the CMT.

To do so, we first compute the nonlinear first-order frequency perturbation due to the total field \mathbf{E} present from all of the modes. Once the frequency perturbations $\delta\omega_k$ are known, we can re-introduce these into the coupled-mode theory by simply setting $\omega_k \rightarrow \omega_k + \delta\omega_k$ in Eq. 1. By comparison with Eqs. 3–6, we can then identify the α and β coefficients.

We consider first a $\chi^{(2)}$ nonlinearity, with the nonlinear polarization $\delta\mathbf{P}$ given by $\delta P_i = \sum_{ijk} \varepsilon \chi_{ijk}^{(2)} E_j E_k$, in a cavity with two modes \mathbf{E}_1 and \mathbf{E}_2 . As before, we require that the modes oscillate with frequency ω_1 and $\omega_2 \approx 2\omega_1$, respectively. Taking $\mathbf{E} = \text{Re}[\mathbf{E}_1 e^{i\omega_1 t} + \mathbf{E}_2 e^{i\omega_2 t}]$ and using the rotating-wave approximation, we can separate the contribution of $\delta\mathbf{P}$ to each $\delta\omega_k$, to obtain the following frequency perturbations:

$$\frac{\delta\omega_1}{\omega_1} = -\frac{1}{4} \frac{\int d^3\mathbf{x} \sum_{ijk} \varepsilon \chi_{ijk}^{(2)} [E_{1i}^* (E_{2j} E_{1k}^* + E_{1j}^* E_{2k})]}{\int d^3\mathbf{x} \varepsilon |\mathbf{E}_1|^2} \quad (8)$$

$$\frac{\delta\omega_2}{\omega_2} = -\frac{1}{4} \frac{\int d^3\mathbf{x} \sum_{ijk} \varepsilon \chi_{ijk}^{(2)} E_{2i}^* E_{1j} E_{1k}}{\int d^3\mathbf{x} \varepsilon |\mathbf{E}_2|^2} \quad (9)$$

Similarly, for a centro-symmetric $\chi^{(3)}$ medium, $\delta\mathbf{P}$ is given by $\delta\mathbf{P} = \varepsilon \chi^{(3)} |\mathbf{E}|^2 \mathbf{E}$, with $\mathbf{E} = \text{Re}[\mathbf{E}_1 e^{i\omega_1 t} + \mathbf{E}_3 e^{i\omega_3 t}]$. We obtain the following frequency perturbations:

$$\frac{\delta\omega_1}{\omega_1} = -\frac{1}{8} \left[\frac{\int d^3\mathbf{x}\varepsilon\chi^{(3)} \left(|\mathbf{E}_1 \cdot \mathbf{E}_1|^2 + 2|\mathbf{E}_1 \cdot \mathbf{E}_1^*|^2 + 2(\mathbf{E}_1 \cdot \mathbf{E}_1^*)(\mathbf{E}_3 \cdot \mathbf{E}_3^*) \right)}{\int d^3\mathbf{x}\varepsilon|\mathbf{E}_1|^2} + \frac{2|\mathbf{E}_1 \cdot \mathbf{E}_3|^2 + 2|\mathbf{E}_1 \cdot \mathbf{E}_3^*|^2 + 3(\mathbf{E}_1^* \cdot \mathbf{E}_1^*)(\mathbf{E}_1^* \cdot \mathbf{E}_3)}{\int d^3\mathbf{x}\varepsilon|\mathbf{E}_1|^2} \right] \quad (10)$$

$$\frac{\delta\omega_3}{\omega_3} = -\frac{1}{8} \left[\frac{\int d^3\mathbf{x}\varepsilon\chi^{(3)} \left(|\mathbf{E}_3 \cdot \mathbf{E}_3|^2 + 2|\mathbf{E}_3 \cdot \mathbf{E}_3^*|^2 + 2(\mathbf{E}_1 \cdot \mathbf{E}_1^*)(\mathbf{E}_3 \cdot \mathbf{E}_3^*) \right)}{\int d^3\mathbf{x}\varepsilon|\mathbf{E}_3|^2} + \frac{2|\mathbf{E}_1 \cdot \mathbf{E}_3|^2 + 2|\mathbf{E}_1 \cdot \mathbf{E}_3^*|^2 + (\mathbf{E}_1 \cdot \mathbf{E}_1)(\mathbf{E}_1 \cdot \mathbf{E}_3^*)}{\int d^3\mathbf{x}\varepsilon|\mathbf{E}_3|^2} \right] \quad (11)$$

There is a subtlety in the application of perturbation theory to decaying modes, such as those of a cavity coupled to output ports. In this case, the modes are not truly eigenmodes, but are rather “leaky modes” [52], and are not normalizable. Perturbative methods in this context are discussed in more detail by [51, 52], but for a tightly confined cavity mode it is sufficient to simply ignore the small radiating field far away from the cavity. The field in the cavity is very nearly that of a true eigenmode of an isolated cavity.

As stated above, we can arrive at the coupling coefficients by setting $\omega_k \rightarrow \omega_k + \delta\omega_k$ in Eq. 1. However, the frequency perturbations $\delta\omega_k$ are time-independent quantities, and we need to connect them to the time-dependent a_k amplitudes. Therefore, to re-introduce the time dependence, one can use the slowly varying envelope approximation: a slowly varying, time-dependent amplitude $a_k(t)$ is introduced into the unperturbed fields $\mathbf{E}_k \rightarrow \mathbf{E}_k a_k(t)$. The eigenmode must be normalized so that $|a_k|^2$ is the energy, as assumed for the coupled-mode theory. Thus, we divide each \mathbf{E}_k by $\sqrt{\frac{1}{2} \int \varepsilon |\mathbf{E}_k|^2}$.

First, we consider the $\chi^{(2)}$ medium. Carrying out the above substitutions in Eq. 1 and grouping terms proportional a_k yields Eqs. 3–4 with α_{ij} and β_i given by:

$$\alpha_{ij} = 0 \quad (12)$$

$$\beta_1 = \frac{1}{4} \frac{\int d^3\mathbf{x} \sum_{ijk} \varepsilon \chi_{ijk}^{(2)} [E_{1i}^* (E_{2j} E_{1k}^* + E_{1j}^* E_{2k})]}{\left[\int d^3\mathbf{x} \varepsilon |\mathbf{E}_1|^2 \right] \left[\int d^3\mathbf{x} \varepsilon |\mathbf{E}_2|^2 \right]^{1/2}} \quad (13)$$

$$\beta_2 = \frac{1}{4} \frac{\int d^3\mathbf{x} \sum_{ijk} \varepsilon \chi_{ijk}^{(2)} E_{2i}^* E_{1j} E_{1k}}{\left[\int d^3\mathbf{x} \varepsilon |\mathbf{E}_1|^2 \right] \left[\int d^3\mathbf{x} \varepsilon |\mathbf{E}_2|^2 \right]^{1/2}} \quad (14)$$

A similar calculation yields the $\chi^{(3)}$ coupled-mode

equations with coefficients given by:

$$\alpha_{ii} = \frac{1}{8} \frac{\int d^3\mathbf{x} \varepsilon \chi^{(3)} (|\mathbf{E}_i \cdot \mathbf{E}_i|^2 + |\mathbf{E}_i \cdot \mathbf{E}_i^*|^2)}{\left[\int d^3\mathbf{x} \varepsilon |\mathbf{E}_i|^2 \right]^2} \quad (15)$$

$$\alpha_{31} = \frac{1}{4} \frac{\int d^3\mathbf{x} \varepsilon \chi^{(3)} (|\mathbf{E}_1|^2 |\mathbf{E}_3|^2 + |\mathbf{E}_1 \cdot \mathbf{E}_3|^2 + |\mathbf{E}_1 \cdot \mathbf{E}_3^*|^2)}{\left[\int d^3\mathbf{x} \varepsilon |\mathbf{E}_1|^2 \right] \left[\int d^3\mathbf{x} \varepsilon |\mathbf{E}_3|^2 \right]} \quad (16)$$

$$\alpha_{13} = \alpha_{31} \quad (17)$$

$$\beta_1 = \frac{3}{8} \frac{\int d^3\mathbf{x} \varepsilon \chi^{(3)} (\mathbf{E}_1^* \cdot \mathbf{E}_1^*)(\mathbf{E}_1^* \cdot \mathbf{E}_3)}{\left[\int d^3\mathbf{x} \varepsilon |\mathbf{E}_1|^2 \right]^{3/2} \left[\int d^3\mathbf{x} \varepsilon |\mathbf{E}_3|^2 \right]^{1/2}} \quad (17)$$

$$\beta_3 = \frac{1}{8} \frac{\int d^3\mathbf{x} \varepsilon \chi^{(3)} (\mathbf{E}_1 \cdot \mathbf{E}_1)(\mathbf{E}_1 \cdot \mathbf{E}_3^*)}{\left[\int d^3\mathbf{x} \varepsilon |\mathbf{E}_1|^2 \right]^{3/2} \left[\int d^3\mathbf{x} \varepsilon |\mathbf{E}_3|^2 \right]^{1/2}} \quad (18)$$

Note that Eqs. 12–18 verify the conditions $\omega_1\beta_1 = \omega_2\beta_2^*$ and $\omega_1\beta_1 = \omega_3\beta_3^*$, previously derived from conservation of energy—for $\chi^{(2)}$, this requires that one apply the symmetries of the $\chi_{ijk}^{(2)}$ tensor, which is invariant under permutations of ijk for a frequency-independent $\chi^{(2)}$ [46]. Furthermore, we can relate the coefficients α and β to an effective modal volume V , similar to Ref. 55. In particular, the strongest possible nonlinear coupling will occur if the eigenfields are a constant in the nonlinear material and zero elsewhere. In this case, any integral over the fields will simply yield the geometric volume V of the nonlinear material. Thus, for the $\chi^{(2)}$ effect we would obtain $\beta_i \sim \chi^{(2)}/\sqrt{V\varepsilon}$; similarly, for the $\chi^{(3)}$ effect we would obtain $\alpha_{ij}, \beta_i \sim \chi^{(3)}/V\varepsilon$. This proportionality to $1/\sqrt{V}$ and $1/V$ carries over to more realistic field profiles (and in fact could be used to *define* a modal volume for these effects).

NUMERICAL VALIDATION

To check the predictions of the $\chi^{(3)}$ coupled-mode equations, we performed an FDTD simulation of the one-dimensional waveguide-cavity system shown in Fig 1, whose analytical properties are uniquely suited to third-harmonic generation. (The FDTD method, including techniques to simulate nonlinear media, is described in Ref. 56.) This geometry consists of a semi-infinite photonic-crystal structure made of alternating layers of dielectric ($\varepsilon_1 = 13$ and $\varepsilon_2 = 1$) with period a and thicknesses given by the quarter-wave condition ($d_1 = \sqrt{\varepsilon_2}/(\sqrt{\varepsilon_1} + \sqrt{\varepsilon_2})$ and $d_2 = a - d_1$, respectively). Such a quarter-wave stack possesses a periodic sequence of photonic band gaps centered on frequencies $\omega_1 = (\sqrt{\varepsilon_1} + \sqrt{\varepsilon_2})/4\sqrt{\varepsilon_1\varepsilon_2}$ (in units of $2\pi c/a$) for the lowest gap, and higher-order gaps centered on odd multiples of ω_1 . Moreover, a defect formed by doubling the thickness of a ε_1 layer creates cavity modes at exactly the middle of every one of these gaps. Therefore, it automatically satisfies the frequency-matching condition for third-harmonic generation. In fact, it is too good: there will also be “ninth harmonic” generation from ω_3 to ω_9 . This unwanted process is removed, however, by the discretization error of the FDTD simulation, which introduces numerical dispersion that shifts the higher-frequency modes. To ensure the $\omega_3 = 3\omega_1$ condition in the face of this dispersion, we slightly perturbed the structure (increasing the dielectric constant slightly at the nodes of the third-harmonic eigenfield) to tune the frequencies. The simulated crystal was effectively semi-infinite, with many more layers on the right than on the left of the cavity. On the left of the cavity, after two period of the crystal the material is simply air ($\varepsilon = 1$), terminated by a perfectly matched layer (PML) absorbing boundary region.

We excite the cavity with an incident plane wave of frequency ω_1 , and compute the resulting reflection spectrum. The reflected power at ω_3 , the third-harmonic generation, was then compared with the prediction of the coupled-mode theory. The frequencies, decay rates, and α and β coefficients in the coupled-mode theory were computed from a linear FDTD simulation in which the eigenmodes were excited by narrow-band pulses. The freely available FDTD code of [57] was employed.

The results are shown in Fig. 2, in which the output power at ω_1 and $\omega_3 = 3\omega_1$ is denoted by $|s_{1-}|^2$ and $|s_{3-}|^2$, respectively, while the input power at ω_1 is denoted by $|s_{1+}|^2$. In particular, we plot convenient dimensionless quantities: the third-harmonic conversion efficiency $|s_{3-}|^2/|s_{1+}|^2$ as a function of the dimensionless product $n_2|s_{1+}|^2$ in terms of the standard Kerr coefficient $n_2 = 3\chi^{(3)}/4c\varepsilon$. There is clear agreement between the FDTD and CMT for small values of $n_2|s_{1+}|^2$ (in which limit the conversion goes quadratically with $n_2|s_{1+}|^2$). However, as the input power in-

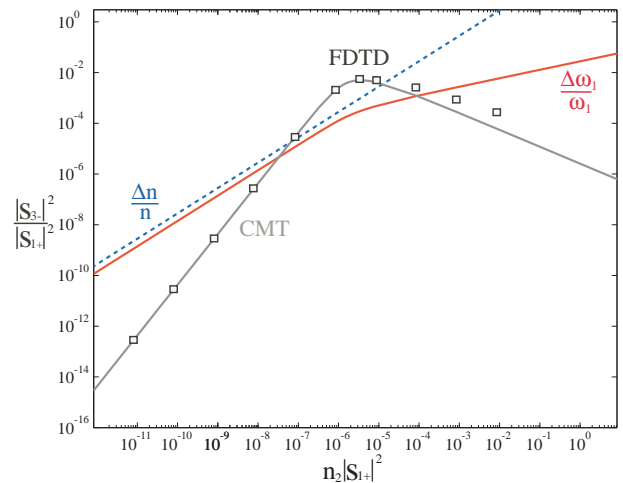


FIG. 2: Log-log plot of $|s_{3-}|^2/|s_{1+}|^2$ vs. $n_2|s_{1+}|^2$ for the coupled-mode theory (grey) and FDTD (black squares), where n_2 is being varied. Also shown are the corresponding $\Delta n/n$ (dashed blue) and $\Delta\omega_1/\omega_1$ (solid red) curves.

creases, they eventually begin to disagree, marking the point where second-order corrections are required. This disagreement is not a practical concern, however, because the onset of second-order effects coincides with the limits of typical materials, which usually break down for $\Delta n/n \equiv \chi^{(3)}\max|E|^2/2\varepsilon > 1\%$. This is why we also plot the maximum index shift $\Delta n/n$ in the same figure.

Also shown in Fig. 2 is a plot of $\Delta\omega_1/\omega_1 = \text{Re}[\delta\omega_1/\omega_1]$. As expected, when $\Delta\omega_1$ is of the order of $1/Q_1 \sim 10^{-3}$, the frequency shift begins to destroy the frequency matching condition, substantially degrading the third-harmonic conversion. (It might seem that $\Delta n/n$ and $\Delta\omega_1/\omega_1$ should be comparable, but this is not the case because $\Delta n/n$ is the maximum index shift while $\Delta\omega_1/\omega_1$ is due to an average index shift.)

More specifically, the details of our simulation are as follows. To simulate a continuous wave (CW) source spectrum in FDTD, we employ a narrow-bandwidth gaussian pulse incident from the air region, which approximates a CW source in the limit of narrow bandwidth. This pulse is carefully normalized so that the peak *intensity* is unity, to match the CMT. The field in the air region is Fourier transformed and subtracted from the incident field to yield the reflected flux. Using only two periods of quarter-wave stack on the left of the cavity we obtained two cavity modes with real frequencies $\omega_1 = 0.31818$ ($2\pi c/a$), $\omega_2 = 0.95454$ ($2\pi c/a$) and quality factors $Q_1 = 1286$ and $Q_3 = 3726$, respectively. Given these field patterns, we computed the α_{ij} and β_i coefficients. We obtained the following coupling coefficients, in units of $\chi^{(3)}/a$: $\alpha_{11} = 4.7531 \times 10^{-4}$, $\alpha_{22} = 5.3306 \times 10^{-4}$, $\alpha_{12} = \alpha_{21} = 2.7847 \times 10^{-4}$, $\beta_1 = (4.55985 - 0.7244i) \times 10^{-5}$.

COMPLETE FREQUENCY CONVERSION

We now consider the conditions under which one may achieve *complete* frequency conversion: 100% of the incident power converted to output at the second or third harmonic frequency. As we shall see, this is easiest to achieve in the $\chi^{(2)}$ case, and requires additional design criteria in the $\chi^{(3)}$ case.

The key fact in a $\chi^{(2)}$ medium is that there are no frequency-shifting terms ($\alpha = 0$), so the resonance condition $\omega_2 = 2\omega_1$ is not spoiled as one increases the power. The only requirement that we must impose is that external losses such as absorption are negligible ($\tau_{e,k} \gg \tau_{s,k}$). In this case, 100% conversion corresponds to setting $s_{1-} = 0$ in the steady-state. Using this fact, Eqs. 3-4 for an input source $s_+(t) = s_{1+} \exp(i\omega_1 t)$ yields the following condition on the input power for 100% conversion:

$$|s_{1+}|^2 = \frac{2}{\omega_1^2 |\beta_1|^2 \tau_{s,2} \tau_{s,1}^2} = \frac{\omega_1}{2 |\beta_1|^2 Q_2 Q_1^2} \quad (19)$$

(A similar dependence of efficiency on $Q_1^2 Q_2$ was previously observed [5, 8], although a critical power was not identified.) Thus, we can always choose an input power to obtain 100% conversion. If $Q_1 \sim Q_2$, then this critical power scales as V/Q^3 where V is the modal volume (recall that $\beta \sim 1/\sqrt{V}$).

This is limited, however, by our first-order approximation in perturbation theory: if the input power becomes so large that second-order effects (or material breakdown) become significant, then this prediction of 100% conversion is no longer valid. The key condition is that the fractional change in the refractive index be small: $\Delta n/n \ll 1$. This can always be satisfied, in principle: if one chooses Q_1 and/or Q_2 to be sufficiently large, then the critical power can be made arbitrarily small in principle. Not only does the critical power decrease with Q^3 , but the field intensity in the cavity ($|a_i|^2$) decreases as $V/Q_1 Q_2$, and thus one can avoid large $\Delta n/n$ as well as lowering the power. (Note that the field intensity goes as $1/Q^2$ while the power goes as $1/Q^3$ simply because the energy and power are related by a time scale of Q .)

To illustrate second-harmonic conversion for a $\chi^{(2)}$ medium, we plot the solution to the coupled-mode equations as a function of input power in Fig. 3. The 100% conversion at the predicted critical power is clearly visible. For this calculation, we chose modal parameters similar to the ones from the FDTD computation before: $\omega_1 = 0.3$, $\omega_2 = 0.6$, $Q_1 = 10^4$, $Q_2 = 2 \times 10^4$, with dimensionless $\beta_1 = (4.55985 - 0.7244) \times 10^{-5}$.

A $\chi^{(3)}$ medium, on the other hand, does suffer from nonlinear frequency shifts. For example, Fig. 2, which is by no means the optimal geometry, exhibits a maximal efficiency of $|s_{3-}|^2/|s_{1+}|^2 \approx 4 \times 10^{-3}$, almost three orders of magnitude away from complete frequency conversion. On the other hand, we can again achieve 100%

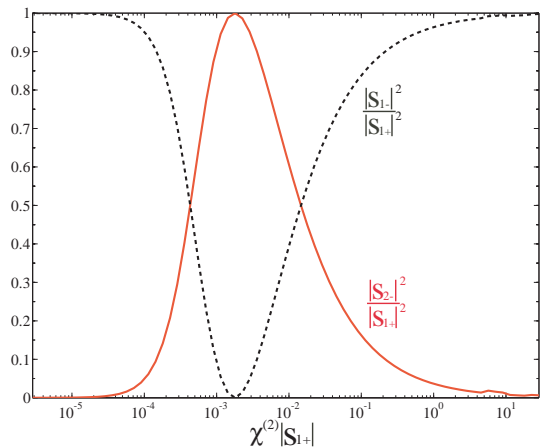


FIG. 3: Plot of first and second harmonic efficiency, $|s_{1-}|^2/|s_{1+}|^2$ (black) and $|s_{2-}|^2/|s_{1+}|^2$ (red), vs. $\chi^{(2)}|s_{1+}|$. 100% power transfer from ω_1 to $\omega_2 = 2\omega_1$ is achieved at $\chi^{(2)}|s_{1+}| = 1.8 \times 10^{-3}$.

conversion if we can force $\alpha_{ij} = 0$, which can be done in two ways. First, one could employ *two* $\chi^{(3)}$ materials with opposite-sign $\chi^{(3)}$ values (e.g., as in Ref. 58). For example, if the $\chi^{(3)}$ is an *odd* function around the cavity center, then the integrals for α_{ij} will vanish while the β integrals will not. (In practice, $\alpha \ll \beta$ should suffice.) Second, one could pre-compensate for the nonlinear frequency shifts: design the cavity so that the shifted frequencies, at the critical power below, satisfy the resonant condition $\omega_3 + \Delta\omega_3 = 3(\omega_1 + \Delta\omega_1)$. Equivalently, design the device for $\alpha_{ij} = 0$ and then adjust the linear cavity frequencies *a posteriori* to compensate for the frequency shift at the critical power. (This is closely analogous to the cavity detuning used for optical bistability [55], in which one operates off-resonance in the linear regime so that resonance occurs from the nonlinear shift.)

If α_{ij} is thereby forced to be zero, and we can also neglect external losses (absorption, etc.) as above, then 100% third-harmonic conversion ($s_{1-} = 0$) is obtained when:

$$|s_{1+}|^2 = \left[\frac{4}{\omega_1^2 |\beta_1|^2 \tau_{s,1}^3 \tau_{s,3}} \right]^{1/2} = \left[\frac{\omega_1 \omega_3}{4 |\beta_1|^2 Q_1^3 Q_3} \right]^{1/2} \quad (20)$$

If $Q_1 \sim Q_3$, then this critical power scales as V/Q^2 where V is the modal volume (recall that $\beta \sim 1/V$). This is precisely the scaling that was predicted for the power to obtain nonlinear bistability in a single-mode cavity [59]. Similarly, one finds that the energy density in the cavity ($|a_i|^2$) decreases proportional to $V/\sqrt{Q_1 Q_3}$.

We demonstrate the third-harmonic conversion for $\alpha_{ij} = 0$ by plotting the solution to the coupled-mode equations as a function of input power in Fig. 4. Again, 100% conversion is only obtained at a single critical power. Here, we used the same parameters as in the

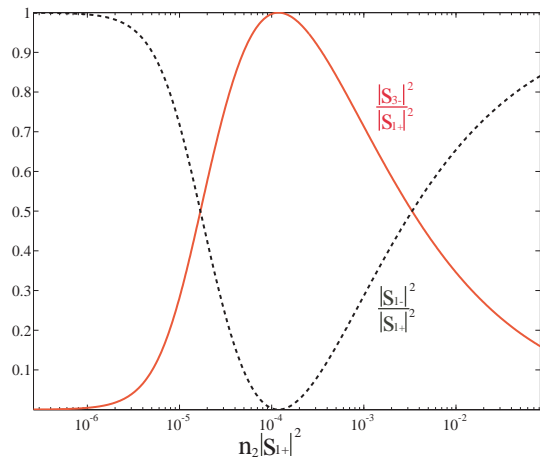


FIG. 4: Plot of first and third harmonic efficiency, $|s_{1-}|^2/|s_{1+}|^2$ (black) and $|s_{3-}|^2/|s_{1+}|^2$ (red), vs. $n_2|s_{1+}|^2$. 100% power transfer from ω_1 to $\omega_3 = 3\omega_1$ is achieved at $n_2|s_{1+}|^2 = 2.8 \times 10^{-4}$.

FDTD calculation, but with $\alpha = 0$. In this case, comparing with Fig. 2, we observe that complete frequency conversion occurs at a power corresponding to $\Delta n/n \approx 10^{-2}$. This is close to the maximum power before coupled-mode/perturbation theory becomes invalid (either because of second-order effects or material breakdown), but we could easily decrease the critical power by increasing Q .

For both the $\chi^{(2)}$ and the $\chi^{(3)}$ effects, in Figs. 3–4, we see that the harmonic conversion efficiency goes to zero if the input power (or χ) is either too small or too large. It is not surprising that frequency conversion decreases for low powers, but the decrease in efficiency for high powers is less intuitive. It corresponds to a well-known phenomenon in coupled-mode systems: in order to get 100% transmission from an input port to an output port, the coupling rates to the two ports must be matched in order to cancel the back-reflected wave [50, 60]. In the present case, the coupling rate to the input port is $\sim 1/Q_1$, and the coupling rate to the output “port” (the harmonic frequency) is determined by the strength of the nonlinear coupling. If the nonlinear coupling is either too small or too large, then the rates are not matched and the light is reflected instead of converted. (On the other hand, we find that for large input powers, while the conversion *efficiency* as a fraction of input power goes to zero, the *absolute* converted power ($|s_{2-}|^2$ or $|s_{3-}|^2$) goes to a constant.)

Finally, let us consider one other potential problem. Any physical $\chi^{(2)}$ medium will generally also have $\chi^{(3)} \neq 0$, so if the power is large enough this could conceivably cause a frequency shift that would spoil the second-harmonic resonance even in the $\chi^{(2)}$ device. Here, we perform a simple scaling analysis to determine when this will occur. (Although the frequency shifting could poten-

tially be compensated for as described above, one prefers that it be negligible to begin with.) In order to preserve the resonance condition, any fractional frequency shift $\Delta\omega/\omega$ must be much smaller than the bandwidth $1/Q$, or equivalently we must have $Q\Delta\omega/\omega \ll 1$. From above, $\Delta\omega \sim \omega\alpha|a|^2$, and $|a|^2 \sim |s_{1+}|^2 Q/\omega$. Suppose that we are operating at the critical input power $P^{(2)}$ for second-harmonic conversion, from Eq. 19. It then follows that we desire $Q\Delta\omega/\omega \sim Q^2\alpha/\omega P^{(2)} \ll 1$. It is convenient to re-express this relationship in terms of $P^{(3)} \sim \omega/\beta Q^2$, the third-harmonic critical power from Eq. 19, by assuming $\alpha \sim \beta$ as discussed in the previous section. We therefore find that $\chi^{(3)}$ self-phase modulation can be ignored for $\chi^{(2)}$ second-harmonic generation as long as $P^{(2)}/P^{(3)} \ll 1$. As discussed in the concluding remarks, this is indeed the case for common materials such as gallium arsenide, where $P^{(2)}/P^{(3)} \approx 1/30$ for $Q \sim 1000$ and for typical values of the cavity lifetime and volume. Moreover, since $P^{(2)}/P^{(3)} \sim 1/Q$, one can make the ratio arbitrarily smaller if necessary (at the expense of bandwidth) by increasing Q .

THE EFFECT OF LOSSES

In practice, a real device will have some additional losses, such as linear or nonlinear absorption and radiative scattering. Such losses will lower the peak conversion efficiency below 100%. As we show in this section, their quantitative effect depends on the ratio of the loss rate to the total loss rate $1/Q$. We also solve for the critical input power to achieve maximal conversion efficiency in the presence of losses.

For a $\chi^{(2)}$ medium with a linear loss rate $1/\tau_{e,k}$, we solve Eqs 3–4 for $|s_{2-}|^2$ and enforce the condition for maximal conversion efficiency: $\frac{d}{d|s_{1+}|^2}(|s_{2-}|^2/|s_{1+}|^2) = 0$. We thus obtain the following optimal input power and conversion efficiency:

$$|s_{1+}|^2 = \frac{2\tau_{s,1}}{\omega_1^2 |\beta_1|^2 \tau_1^3 \tau_2} \quad (21)$$

$$\frac{|s_{2-}|^2}{|s_{1+}|^2} = \frac{\tau_1 \tau_2}{\tau_{s,1} \tau_{s,2}} \quad (22)$$

It immediately follows that for zero external losses, i.e. $\tau_k = \tau_{s,k}$, Eq. 22 gives 100% conversion and Eq. 21 reduces to Eq. 19. For small external losses $\tau_{s,k} \ll \tau_{e,k}$, the optimal efficiency is reduced by the ratio of the loss rates, to first order:

$$\frac{|s_{2-}|^2}{|s_{1+}|^2} \approx 1 - \left(\frac{\tau_{s,2}}{\tau_{e,2}} + \frac{\tau_{s,1}}{\tau_{e,1}} \right). \quad (23)$$

(A similar transmission reduction occurs in coupled-mode theory when any sort of loss is introduced into a resonant coupling process [54].)

The same analysis for $\chi^{(3)}$ yields the following critical input power and optimal efficiency:

$$|s_{1+}|^2 = \left[\frac{4\tau_{s,1}^2}{\omega_1^2 |\beta_1|^2 \tau_1^5 \tau_3} \right]^{1/2} \quad (24)$$

$$\frac{|s_{3-}|^2}{|s_{1+}|^2} = \frac{\tau_1 \tau_3}{\tau_{s,1} \tau_{s,3}} \quad (25)$$

where by comparison with Eq. 22, a first-order expansion for low-loss yields an expression of the same form as Eq. 23: the efficiency is reduced by the ratio of the loss rates, with τ_2 replaced by τ_3 .

A $\chi^{(3)}$ medium may also have a nonlinear “two-photon” absorption, corresponding to a complex-valued $\chi^{(3)}$, which gives an absorption coefficient proportional to the field intensity. This enters the coupled-mode equations as a small imaginary part added to α , even if we have set the real part of α to zero. (The corresponding effect on β is just a phase shift.) That yields a nonlinear (NL) $\tau_{e,k}$ of the following form, to lowest order in the loss:

$$\frac{1}{\tau_{e,1}^{\text{NL}}} \approx \omega_1 \text{Im} \left[\alpha_{11} \frac{\tau_{s,1}}{2} |s_{1+}|^2 + \alpha_{13} \frac{\tau_{s,3}^2 \tau_{s,1}^3}{8} \omega_3^2 |\beta_3|^2 |s_{1+}|^6 \right] \quad (26)$$

$$\frac{1}{\tau_{e,3}^{\text{NL}}} \approx \omega_3 \text{Im} \left[\alpha_{31} \frac{\tau_{s,1}}{2} |s_{1+}|^2 + \alpha_{33} \frac{\tau_{s,3}^2 \tau_{s,1}^3}{8} \omega_3^2 |\beta_3|^2 |s_{1+}|^6 \right]. \quad (27)$$

where we have simply substituted the values for the critical fields $a_1 = \sqrt{2/\tau_1} s_{1+}$ and a_3 given by Eq. 6, and grouped terms that correspond to imaginary frequency shifts. These loss rates can then be substituted in the expression for the losses above, i.e. Eq. 25, in which case one obtains the following optimal efficiency of third-harmonic generation, to lowest-order in the loss, not including linear losses:

$$\frac{|s_{3-}|^2}{|s_{1+}|^2} \approx 1 - \frac{\tau_{s,3}}{|\beta_1|} \sqrt{\frac{\tau_{s,3}}{\tau_{s,1}}} \text{Im} \left[\frac{\alpha_{11} + 3\alpha_{13}}{\tau_{s,3}} + \frac{\alpha_{13} + 3\alpha_{33}}{\tau_{s,1}} \right] \quad (28)$$

(The linear and nonlinear losses can be combined by simply multiplying Eq. 25 and Eq. 28.) Thus, the nonlinear loss is proportional to the ratio $\text{Im} \alpha / |\beta|$, which is proportional to $\text{Im} \chi^{(3)} / |\chi^{(3)}|$.

CONCLUSION

We have presented a rigorous coupled-mode theory for second- and third-harmonic generation in doubly resonant nonlinear cavities, accurate to first order in the nonlinear susceptibility and validated against a direct FDTD simulation. Our theory, which generalizes previous work

on this subject, predicts several interesting consequences. First, it is possible to design the cavity to yield 100% frequency conversion in a passive (gain-free) device, even when nonlinear down-conversion processes are included, limited only by fabrication imperfections and losses. Second, this 100% conversion requires a certain critical input power—powers either too large or too small lead to lower efficiency. Third, we describe how to compensate for the self-phase modulation in a $\chi^{(3)}$ cavity. The motivation for this work was the hope that a doubly resonant cavity would lead to 100% conversion at very low input powers, and so we conclude our paper by estimating the critical power for reasonable material and geometry assumptions.

A typical nonlinear material is gallium arsenide (GaAs), with $\chi^{(2)} \approx 145$ pm/V and $n_2 = 1.5 \times 10^{-13}$ cm²/W at 1.5 μ m. (Al doping is usually employed to decrease nonlinear losses near resonance [61].) Although this has both $\chi^{(2)}$ and $\chi^{(3)}$ effects, we can selectively enhance one or the other by choosing the cavity to have resonances at either the second or third harmonic. Many well confined optical cavity geometries are available at these wavelengths and have been used for nonlinear devices, such as ring resonators [62] or photonic-crystal slabs [63]. We will assume conservative parameters for the cavity: a lifetime $Q_1 = 1000$, $Q_2 = 2000$, $Q_3 = 3000$, and a modal volume of 10 cubic half-wavelengths ($V \approx 10(\lambda/2n)^3$) with roughly constant field amplitude in the nonlinear material (worse than a realistic case of strongly peaked fields). In this case, the critical input power, from Eqs. 19–20, becomes approximately 70 μ W for second-harmonic generation and 2 mW for third-harmonic generation (with a moderate peak index shift $\Delta n/n \approx 10^{-3}$, justifying our first-order approximation)

Future work will involve designing specific doubly resonant cavity geometries and more precise power predictions. Using our expressions for α and β , optimized cavities for harmonic generation can be designed using standard methods to compute the linear eigenmodes. In practice, experimentally achieving cavity modes with “exactly” harmonic frequencies, matched to within the fractional bandwidth $1/Q$, is a challenge and may require some external tuning mechanism. For example, one could use the nonlinearity itself for tuning, via external illumination of the cavity with an intense “tuning” beam at some other frequency. Also, although we can directly integrate the coupled-mode equations in time, we intend to supplement this with a linearized stability analysis at the critical power. This is particularly important for the $\chi^{(3)}$ case, where pre-correcting the frequency to compensate the nonlinear frequency shift (self-phase modulation) may require some care to ensure a stable solution.

Acknowledgements

We would like to thank Zheng Wang and Karl Koch for useful discussions, as well as the anonymous referees for many helpful suggestions. This work was supported in part by the Materials Research Science and Engineering Center program of the National Science Foundation under award DMR-9400334, by a Department of Energy (DOE) Computational Science Fellowship under grant DE-FG02-97ER25308, and also by the Paul E. Gray Undergraduate Research Opportunities Program Fund at MIT.

* Electronic address: alexrod7@mit.edu

- [1] P. D. Drummond, K. J. McNeil, and D. F. Walls, “Nonequilibrium transitions in sub/second harmonic generation I: Semiclassical theory,” *Optica Acta.* **27**(3), 321–335 (1980).
- [2] L.-A. Wu, M. Xiao, and H. J. Kimble, “Squeezed states of light from an optical parametric oscillator,” *JOSA-B* **4**, 1465–1476 (1987).
- [3] Z. Y. Ou and H. J. Kimble, “Enhanced conversion efficiency for harmonic generation with double resonance,” *Opt. Lett.* **18**, 1053–1055 (1993).
- [4] R. Paschotta, K. Fiedler, P. Kurz, and J. Mlynek, “Nonlinear mode coupling in doubly resonant frequency doublers,” *Appl. Phys. Lett.* **58**, 117 (1994).
- [5] V. Berger, “Second-harmonic generation in monolithic cavities,” *J. Opt. Soc. Am. B* **14**, 1351 (1997).
- [6] I. I. Zootoverkh, K. N. V., and E. G. Lariontsev, “Enhancement of the efficiency of second-harmonic generation in microlaser,” *Quantum Electron.* **30**, 565 (2000).
- [7] B. Maes, P. Bienstman, and R. Baets, “Modeling second-harmonic generation by use of mode expansion,” *J. Opt. Soc. Am. B* **22**, 1378 (2005).
- [8] M. Liscidini and L. A. Andreani, “Second-harmonic generation in doubly resonant microcavities with periodic dielectric mirrors,” *Phys. Rev. E* **73**, 016,613 (2006).
- [9] Y. Dumeige and P. Feron, “Whispering-gallery-mode analysis of phase-matched doubly resonant second-harmonic generation,” *PRA* **74**, 063,804 (2006).
- [10] G. T. Moore, K. Koch, and E. C. Cheung, “Optical parametric oscillation with intracavity second-harmonic generation,” *Opt. Commun.* **113**, 463 (1995).
- [11] M. Liscidini and L. A. Andreani, “Highly efficient second-harmonic generation in doubly resonant planar microcavities,” *Appl. Phys. Lett.* **85**, 1883 (2004).
- [12] L. Fan, H. Ta-Chen, M. Fallahi, J. T. Murray, R. Bedford, Y. Kaneda, J. Hader, A. R. XZakharian, J. Moloney, S. W. Koch, and W. Stolz, “Tunable watt-level blue-green vertical-external-cavity surface-emitting lasers by intracavity frequency doubling,” *Appl. Phys. Lett.* **88**, 2251,117 (2006).
- [13] P. Scotto, P. Colet, and M. San Miguel, “All-optical image processing with cavity type II second-harmonic generation,” *Opt. Lett.* **28**, 1695 (2003).
- [14] G. McConnell, A. I. Ferguson, and N. Langford, “Cavity-augmented frequency tripling of a continuous wave mode-locked laser,” *J. Phys. D: Appl. Phys.* **34**, 2408 (2001).
- [15] G. S. Dutta and J. Jolly, “Third harmonic generation in layered media in presence of optical bistability of the fundamental,” *Pramana J. Phys.* **50**, 239 (1988).
- [16] G. D. Aguanno, M. Centini, M. Scalora, C. Sibilia, M. Bertolotti, M. J. Bloemer, and C. M. Bowden, “Generalized coupled-mode theory for $\chi^{(2)}$ interactions in finite multi-layered structures,” *J. Opt. Soc. Am. B* **19**, 2111–2122 (2002).
- [17] A. R. Cowan and J. F. Young, “Mode matching for second-harmonic generation in photonic crystal waveguides,” *Phys. Rev. E* **65**, 085,106 (2002).
- [18] A. M. Malvezzi, G. Vecchi, M. Patrini, G. Guizzetti, L. C. Andreani, F. Romanato, L. Businaro, E. D. Fabrizio, A. Passaseo, and M. D. Vittorio, “Resonant second-harmonic generation in a GaAs photonic crystal waveguide,” *Phys. Rev. B* **68**, 161,306 (2003).
- [19] S. Pearl, H. Lotem, and Y. Shimony, “Optimization of laser intracavity second-harmonic generation by a linear dispersion element,” *J. Opt. Soc. Am. B* **16**, 1705 (1999).
- [20] A. V. Balakin, V. A. Bushuev, B. I. Mantsyzov, I. A. Ozheredov, E. V. Petrov, and A. P. Shkurinov, “Enhancement of sum frequency generation near the photonic band edge under the quasiphase matching condition,” *Phys. Rev. E* **63**, 046,609 (2001).
- [21] G. D. Aguanno, M. Centini, M. Scalora, C. Sibilia, Y. Dumeige, P. Vidavovic, J. A. Levenson, M. J. Bloemer, C. M. Bowden, J. W. Haus, and M. Bertolotti, “Photonic band edge effects in finite structures and applications to $\chi^{(2)}$ interactions,” *Phys. Rev. E* **64**, 016,609 (2001).
- [22] A. H. Norton and C. M. de Sterke, “Optimal poling of nonlinear photonic crystals for frequency conversion,” *Opt. Lett.* **28**, 188 (2002).
- [23] J. A. Armstrong, N. loembergen, J. Ducuing, and P. S. Pershan, “Interactions between light waves in a nonlinear dielectric,” *Phys. Rev.* **127**, 1918–1939 (1962).
- [24] A. Ashkin, G. D. Boyd, and J. M. Dziedzic, “Resonant optical second harmonic generation and mixing,” *IEEE J. Quantum Electron.* **2**, 109–124 (1966).
- [25] R. G. Smith, “Theory of intracavity optical second-harmonic generation,” *IEEE J. Quantum Electron.* **6**, 215–223 (1970).
- [26] A. I. Gerguson and M. H. Dunn, “Intracavity second harmonic generation in continuous-wave dye lasers,” *IEEE J. Quantum Electron.* **13**, 751–756 (1977).
- [27] M. Brieger, H. Busener, A. Hese, F. V. Moers, and A. Renn, “Enhancement of single frequency SHG in a passive ring resonator,” *Opt. Commun.* **38**, 423–426 (1981).
- [28] J. C. Berquist, H. Hemmati, and W. M. Itano, “High power second harmonic generation of 257 nm radiation in an external ring cavity,” *Opt. Commun.* **43**, 437–442 (1982).
- [29] W. J. Kozlovsky, W. P. Risk, W. Lenth, B. G. Kim, G. L. Bona, H. Jaeckel, and D. J. Webb, “Blue light generation by resonator-enhanced frequency doubling of an extended-cavity diode laser,” *Appl. Phys. Lett.* **65**, 525–527 (1994).
- [30] G. J. Dixon, C. E. Tanner, and C. E. Wieman, “432-nm source based on efficient second-harmonic generation of GaAlAs diode-laser radiation in a self-locking external resonant cavity,” *Opt. Lett.* **14**, 731–733 (1989).
- [31] M. J. Collet and R. B. Levien, “Two-photon loss model

- of intracavity second-harmonic generation,” PRA **43**(9), 5068–5073 (1990).
- [32] M. A. Persaud, J. M. Tolchard, and A. I. Ferguson, “Efficient generation of picosecond pulses at 243 nm,” IEEE J. Quantum Electron. **26**, 1253–1258 (1990).
- [33] K. Schneider, S. Schiller, and J. Mlynek, “1.1-W single-frequency 532-nm radiation by second-harmonic generation of a miniature Nd:YAG ring laser,” Opt. Lett. **21**, 1999–2001 (1996).
- [34] X. Mu, Y. J. Ding, H. Yang, and G. J. Salamo, “Cavity-enhanced and quasiphase-matched mutli-order reflection-second-harmonic generation from GaAs/AlAs and GaAs/AlGaAs multilayers,” Appl. Phys. Lett. **79**, 569 (2001).
- [35] J. Hald, “Second harmonic generation in an external ring cavity with a Brewster-cut nonlinear crystal: theoretical considerations,” Opt. Commun. **197**, 169 (2001).
- [36] T. V. Dolgova, A. I. Mailykovski, M. G. Martemyanov, A. A. Fedyanin, O. A. Aktsipetrov, G. Marowsky, V. A. Yakovlev, G. Mattei, N. Ohta, and S. Nakabayashi, “Giant optical second-harmonic generation in single and coupled microcavities formed from one-dimensional photonic crystals,” J. Opt. Soc. Am. B **19**, 2129 (2002).
- [37] T.-M. Liu, C.-T. Yu, and C.-K. Sun, “2 Ghz repetition-rate femtosecond blue sources by second-harmonic generation in a resonantly enhanced cavity,” Appl. Phys. Lett. **86**, 061,112 (2005).
- [38] L. Scaccabarozzi, M. M. Fejer, Y. Huo, S. Fan, X. Yu, and J. S. Harris, “Enhanced second-harmonic generation in AlGaAs/Al_xO_y tightly confining waveguides and resonant cavities,” OL **31**(24), 3626–3630 (2006).
- [39] A. Di Falco, C. Conti, and G. Assanto, “Impedance matching in photonic crystal microcavities for second-harmonic generation,” Opt. Lett. **31**, 250 (2006).
- [40] H. Schnitzler, U. Fröhlich, T. K. W. Boley, A. E. M. Clemen, J. Mlynek, A. Peters, and S. Schiller, “All-solid-state tunable continuous-wave ultraviolet source with high spectral purity and frequency stability,” Appl. Opt. **41**, 7000–7005 (2002).
- [41] F.-F. Ren, R. Li, C. Cheng, and H.-T. Wang, “Giant enhancement of second harmonic generation in a finite photonic crystal with a single defect and dual-localized modes,” PRB **70**, 245,109 (2004).
- [42] K. Koch and G. T. Moore, “Singly resonant cavity-enhanced frequency tripling,” J. Opt. Soc. Am. B **16**, 448 (1999).
- [43] P. P. Markowicz, H. Tiryaki, H. Pudavar, P. N. Prasad, N. N. Lepeshkin, and R. W. Boyd, “Dramatic enhancement of third-harmonic generation in three-dimensional photonic crystals,” Phys. Rev. Lett. **92**(083903) (2004).
- [44] G. I. Stegeman, M. Sheik-Bahae, E. Van Stryland, and G. Assanto, “Large nonlinear phase shifts in second-order nonlinear-optical processes,” Opt. Lett. pp. 13–15 (1993).
- [45] J. D. Joannopoulos, R. D. Meade, and J. N. Winn, *Photonic Crystals: Molding the Flow of Light* (Princeton Univ. Press, 1995).
- [46] R. W. Boyd, *Nonlinear Optics* (Academic Press, California, 1992).
- [47] A. Yariv, *Quantum Electronics, 3rd ed.* (Wiley, New York, 1998).
- [48] D. S. Bethune, “Optical harmonic generation and mixing in multilayer media: analysis using optical transfer matrix techniques,” J. Opt. Soc. Am. B **6**, 910–916 (1989).
- [49] N. Hashizume, M. Ohashi, T. Kondo, and R. Ito, “Optical harmonic generation in multilayered structures: a comprehensive analysis,” J. Opt. Soc. Am. B **12**, 1894–1904 (1995).
- [50] H. A. Haus, *Waves and Fields in Optoelectronics* (Prentice-Hall, Englewood Cliffs, NJ, 1984). Ch. 7.
- [51] W. Suh, Z. Wang, and S. Fan, “Temporal coupled-mode theory and the presence of non-orthogonal modes in lossless multimode cavities,” IEEE J. Quantum Electron. **40**(10), 1511–1518 (2004).
- [52] A. W. Snyder and J. D. Love, *Optical Waveguide Theory* (Chapman and Hall, London, 1983).
- [53] L. D. Landau and E. M. Lifshitz, *Quantum Mechanics*, 3rd ed. (Butterworth-Heinemann, Oxford, 1977).
- [54] H. A. Haus, *Waves and Fields in Optoelectronics* (Prentice-Hall, Englewood Cliffs, NJ, 1984).
- [55] M. Soljačić, M. Ibanescu, S. G. Johnson, Y. Fink, and J. D. Joannopoulos, “Optimal bistable switching in nonlinear photonic crystals,” Phys. Rev. E Rapid Commun. **66**, 055,601(R) (2002).
- [56] A. Taflove and S. C. Hagness, *Computational Electrodynamics: The Finite-Difference Time-Domain Method* (Artech, Norwood, MA, 2000).
- [57] A. Farjadpour, D. Roundy, A. Rodriguez, M. Ibanescu, P. Bermel, J. Burr, J. D. Joannopoulos, and S. G. Johnson, “Improving accuracy by subpixel smoothing in the finite-difference time domain,” Opt. Lett. **31**, 2972–2974 (2006).
- [58] D. D. Smith, G. Fischer, R. W. Boyd, and D. A. Gregory, “Cancellation of photoinduced absorption in metal nanoparticle composites through a counterintuitive consequence of local field effects,” J. Opt. Soc. Am. B **14**, 1625 (1997).
- [59] M. F. Yanik, S. Fan, M. Soljačić, , J. D. Joannopoulos, and Yanik, “All-optical transistor action with bistable switching in a photonic crystal cross-waveguide geometry,” Opt. Lett. **68**, 2506 (2004).
- [60] S. Fan, S. G. Johnson, J. D. Joannopoulos, C. Manolatos, and H. A. Haus, “Waveguide branches in photonic crystals,” J. Opt. Soc. Am. B **18**(2), 162–165 (2001).
- [61] A. Villeneuve, C. C. Yang, G. I. Stegeman, C. Lin, and H. Lin, “Nonlinear refractive-index and two-photon absorption near half the band gap in AlGaAs,” Appl. Phys. Lett. **62**, 2465–2467 (1993).
- [62] Q. Xu and M. Lipson, “Carrier-induced optical bistability in Silicon ring resonators,” Opt. Lett. **31**(3), 341–343 (2005).
- [63] M. Notomi, A. Shinya, S. Mitsugi, G. Kira, E. Kuramochi, and T. Tanabe, “Optical bistable switching action of Si high-Q photonic-crystal nanocavities,” Opt. Express **13**(7), 2678–2687 (2005).